Observation of Molecular and Atomic Ions in Recombination Plasma

A. TONEGAWA, H. MASUMOTO, T. NISHIJIMA, M. ONO and K. KAWAMURA

Department of Physics, School of Science, Tokai University

(Received 5 December 2006 / Accepted 28 May 2007)

Measurements of the densities of the molecular and atomic ions ($n_{H}{}^{+}$, $n_{H2}{}^{+}$, $n_{H3}{}^{+}$) were carried out in hydrogen recombination plasma in the linear divertor plasma simulator, TPD-SheetIV. The molecular and atomic ion currents were detected using an omegatron mass analyzer. The ground-state vibrational temperature of hydrogen molecules T_{vib} is obtained by measurement with VUV emission spectroscopy. Taking into account of T_{vib}, a zero-dimensional model using the relevant rate balance equations was found to predict the observed dominant ion.

Keywords: atomic and molecular process, recombination, omegatron mass analyzer, vibrational temperature, TPD–SheetIV

DOI: 10.1585/pfr.2.S1079

1. Introduction

The production mechanism of atomic and molecular processes in hydrogen plasma has become increasingly important for plasma processing, space plasma, and fusion reactors. In a recombination plasma at low temperature, vibrationally excited hydrogen molecules H_2(v) persist in dissociation and ionization processes of the plasma volume. Thus, the plasma volume recombination associated with H_2(v) molecules in the recombination plasma is effective in enhancing the reduction of ion particle flux [1,2]. The H_2(v) molecules contribute to plasma volume recombination owing to the following chain reactions: H_2(v) + $H^+ \Rightarrow H_2^+$ + H followed by H_2^+ + e $\Rightarrow$ H + H (dissociative recombination: DR) or $H_2^+ + H_2 \Rightarrow H_3^+$ + H.

However, the role of molecular ions in the hydrogen plasma is still under discussion [3–7]. It was shown in a previous paper that the role of molecular ions in the hydrogen plasma for lower plasma density has been done by E.M. Hollmann *et al.* [4] On the other hand, it has been pointed out that even the contribution of recombination is not critical for a reduction in ion flux [8]. Recently, it has been reported that in a typical high-density plasma, H_2(v) molecules assist dissociation (MAD) and ionization (MAI) before they contribute to recombination [9]. For high-density and low-temperature plasma, the MAD always dominates DR. It is thus required that experiments which will aid the understanding of the role of DR are carried out. Molecular processes with H_2(v) molecules have not been reported clearly for high-density plasma.

In this study, we have carried out the experimental observation and modeling of molecular ions in hydrogen plasma in a linear plasma device, TPD-SheetIV [5, 6]. Measurements of the densities of molecular and atomic ions were carried out in hydrogen plasma with a hydrogen gas puff. The molecular and atomic ion currents were detected using an omegatron mass analyzer [7], while the electron density and temperature were measured using a Langmuir probe and a double probe. The ground-state vibrational temperature of hydrogen molecules T_{vib} is obtained by measurement with VUV emission spectroscopy. The zero-dimensional plasma model used to predict the measured densities of hydrogen ion species is discussed.

author's e-mail: tone@keyaki.cc.u-tokai.ac.jp

2. Experimental Apparatus and Method

The experiment was performed in the linear plasma device TPD-SheetIV, shown in Fig. 1 [5, 6]. Ten rectangular magnetic coils formed a uniform magnetic field of 0.8 kG in the experimental region. The hydrogen plasma was generated at a hydrogen gas flow of 75 sccm, with a discharge current of 30-100 A. The neutral pressure P in the experimental region was controlled between 0.1 and 20 mTorr with a secondary gas feed. The sheet plasma flowed from the plasma source along the magnetic field to an endplate located about 1.0 m downstream. Electron density and electron temperature were measured using a planar Langmuir probe and double probe, which were located 3 cm in front of the endplate.

An omegatron mass analyzer, situated behind a small hole (Φ 0.5 mm) in the endplate with a differential pumping system, is used for analyzing ion species [4, 7]. The omegatron mass analyzer is electrically isolating and is water-cooled to allow the entire housing to be inserted into the plasma column. Inside the diagnostic body of this mass analyzer, electrons are stripped away from the particle beam with a pair of electron repeller grids, which are typically dc-biased to $V_e \approx -150$ V. The resulting ion

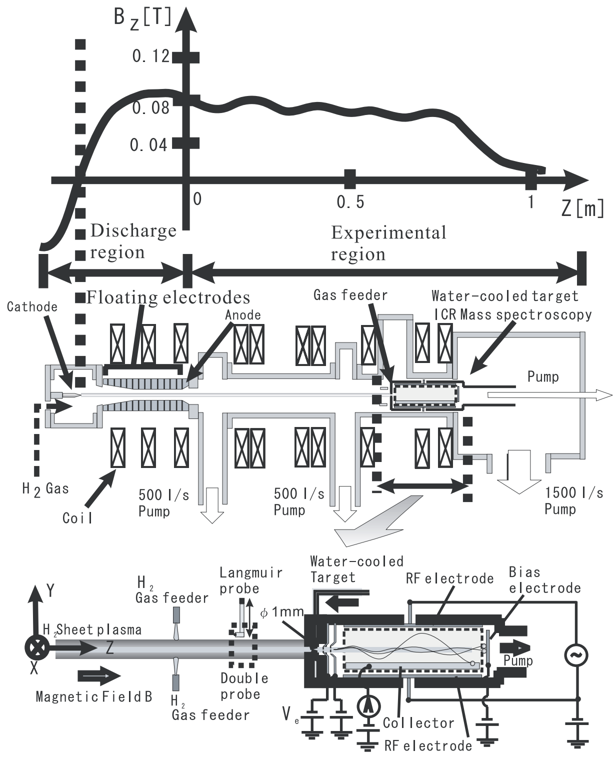

Fig. 1 Schematic diagram of the magnetized plasma simulator (sheet plasma device) TPD-SheetIV and omegatron mass-analyzer.

beam is then slowed by an ion repeller grid and an RF chamber which are dc biased to have slightly higher than the plasma potential. The relative densities of the molecular and atomic ions were determined from the collector current of the mass analyzer. The peaks appear in the collector current of the analyzer when the frequency of the applied RF electric field is equal to the ion cyclotron frequency $f_c \equiv eB/2\pi m$. The current of an ion species j entering the collector should be proportional to the corresponding ion peak current $I_{p,j} \approx en_j \upsilon_{t,j} S$, where $\upsilon_{t,j}$ is the thermal velocity, and S is the area of the small hole in the endplate.

To model the ion density in this experiment, a simple zero-dimensional model is developed for solving the system of rate balance equations for ion and gas species [4, 7, 10]. The processes included in the model are

$$\mathrm{H + e \rightarrow H^+ + 2e,} \quad \text{(el)}$$
$$\mathrm{H_2 + e \rightarrow 2H + e,} \quad \text{(eD)}$$
$$\mathrm{H_2 + e \rightarrow H + H^* + e,} \quad \text{(eDn)}$$
$$\mathrm{H_2(v) + H^+ \rightarrow H_2^+ + H,} \quad \text{(CNV)}$$
$$\mathrm{H_2 + e \rightarrow H_2^+ + e,} \quad \text{(eI2)}$$
$$\mathrm{H_2 + e \rightarrow H^+ + H + 2e,} \quad \text{(eDI)}$$
$$\mathrm{H_2^+ + e \rightarrow H^* + H,} \quad \text{(DR2)}$$
$$\mathrm{H_2^+ + e \rightarrow H^+ + H + e,} \quad \text{(eD2)}$$
$$\mathrm{H_2^+ + e \rightarrow 2H^+ + 2e,} \quad \text{(eDI2)}$$
$$\mathrm{H_2^+ + H_2 \rightarrow H_3^+ + H,} \quad \text{(CNV2)}$$
$$\mathrm{H_3^+ + e \rightarrow H_2^+ + H + e,} \quad \text{(eD3)}$$
$$\mathrm{H_3^+ + e} \rightarrow \begin{cases} 3H \\ H_2 + H, \end{cases} \quad \text{(DR3)}$$
$$\mathrm{H_3^+ + H \rightarrow H_2^+ + H_2.} \quad \text{(BCNV2)}$$

Here, we have ignored radiative and three-body recombination, as well as dissociative electron attachment (H^- formation), as these reactions are believed to be negligible for the conditions studied here. The particle H^* refers to electronically excited atomic hydrogen. In the H_3^+ recombination reaction (DR3), we have assumed a 50% branching ratio between the two reaction channels [11]. For the purposes of calculating the average velocities $\langle \sigma\upsilon \rangle$, the neutral velocities are assumed to be negligible compared with the ion and electron velocities. The ion temperatures are taken to be $T_j = T_e$ (j = 1,2,3), where T_e is the electron temperature. The molecular ion density of H^+, H_2^+, and H_3^+ are described by the steady-state rate balance equations with the charge neutrality $n_e = \sum_j n_j$ [4]. The neutral densities of hydrogen molecules is obtained from the measured neutral gas pressure P. In evaluating the rate coefficients, the reactions involving H_2, H_2^+, and H_3^+ are vibrationally resolved in the model. These rate coefficients are calculated by the available cross-section data [4, 10–13].

We obtain the distribution of ground-state quantum numbers from measured relative intensities of the H_2 molecular radiation between the upper electronic state $B^1\Sigma_u^+(\upsilon')$ and $C^1\Pi_u(\upsilon')$ with vibrational level [14, 15]. The corona model used to calculate the population distribution of the vibrational levels resulting from a Boltzmann population distribution in the ground state characterized by a temperature of hydrogen molecule. Assuming a thermal (Boltzmann) population of ground state ($X^1\Sigma_g^+$) vibrational levels, and given the Franck-Condon matrix for electron-impact excitation from the ground state to the upper state, a ground-state vibrational temperature of hydrogen molecule T_{vib} can be found which results in a best fit to the observed relative intensities of VUV spectrum.

3. Experimental Results

Figure 2 shows the ion densities (n_{H^+}, n_{H2^+}, and n_{H3^+}), the electron density n_e, and the electron temperature T_e plotted against hydrogen gas pressure P at the discharge current I_d of 50 A. Using a small amount of secondary hydrogen gas puffing into a hydrogen plasma, n_e has a maximum value of $5.0 \times 10^{18}\,\mathrm{m^{-3}}$ at $P \sim 4$ mtorr and T_e decreases rapidly from 11 to 3 eV owing to ionization. Above $P \sim 4$ mtorr, T_e falls below 3 eV, and n_e gradually decreases. n_{H^+} shows the same tendency as the characteristics of n_e with increasing P and has a maximum value of $\sim 4.5 \times 10^{18}\,\mathrm{m^{-3}}$ at $P \sim 4$ mtorr. On the other hand, n_{H2^+} and n_{H3^+} decrease and have a minimum values of ∼ 2.0-$3.0 \times 10^{17}\,\mathrm{m^{-3}}$ at $P \sim 4$ mtorr. After that, n_{H2^+} and n_{H3^+} have a maximum value at $P \sim 6$ mtorr and decrease with increasing P.

By defining the ion density ratio as the individual val-

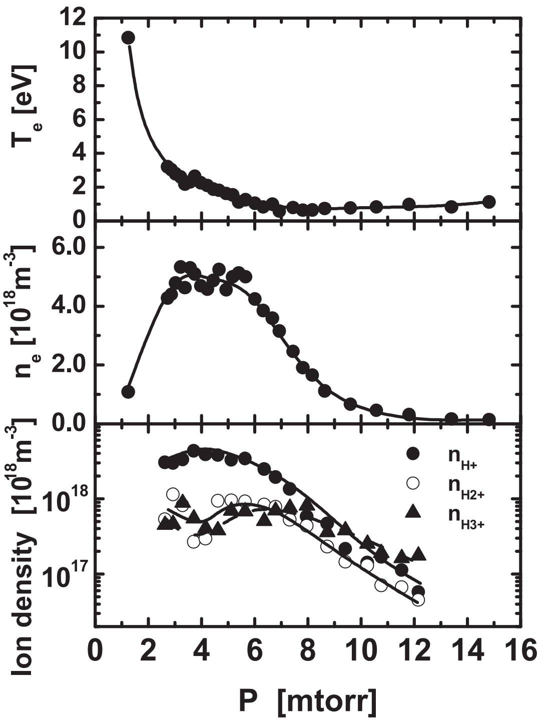

Fig. 2 The ion densities (n_{H^+}, n_{H2^+}, and n_{H3^+}), the electron density n_e, and the electron temperature T_e plotted against hydrogen gas pressure P at the discharge current I_d of 50 A in hydrogen plasma.

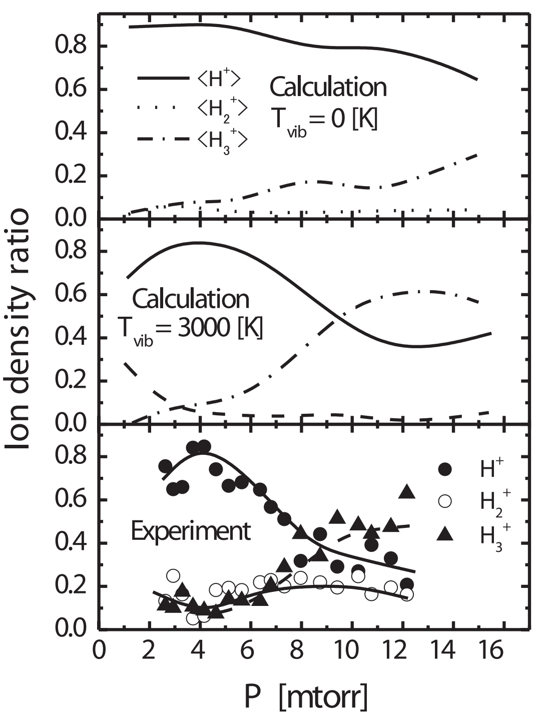

Fig. 3 Measured the ion densities ratio (H^+, H_2^+, and H_3^+), and the calculated ion densities ratio ($\langle H^+\rangle$, $\langle H_2^+\rangle$, and $\langle H_3^+\rangle$) plotted against gas pressure P at the discharge current I_d of 50 A in the hydrogen plasma.

ues of the ion densities divided by the sum of the densities of H^+, H_2^+, and H_3^+, we can express the effect of molecular processes on the hydrogen plasma. Figure 3 shows the measured ion densities ratio (H^+, H_2^+, and H_3^+) and the calculated ion densities ratio ($\langle H^+\rangle$, $\langle H_2^+\rangle$, and $\langle H_3^+\rangle$) plotted against gas pressure P at the discharge current I_d of 50 A in the hydrogen plasma. In the reactions involving H_2, H_2^+, a ground-state vibrational temperature of hydrogen molecule are $T_{vib} = 0$ K and $T_{vib} \sim 3000$ K in the model. The ion density ratio of H^+ is larger than that of H_2^+ or H_3^+ in the low gas pressure (< 6 mtorr), With increasing P, the ion density ratio of H^+ has a maximum value of 0.8 at $P \sim 4$ mtorr and gradually decreases from 0.8 to 0.4. On the other hand, the ion density ratio of H_3^+ rapidly increases from 0.1 to 0.5 with increasing P and saturated up to $P \sim 10$ mtorr. The density ratio of H_2^+ remains nearly constant at around 0.1-0.2 with increasing P. In case of $T_{vib} = 3000$ K in the reactions involving H_2, H_2^+, the characteristic of $\langle H^+\rangle$, $\langle H_2^+\rangle$, and $\langle H_3^+\rangle$ show the same tendency as that of the measured ion density ratio. $\langle H^+\rangle$ has a maximum value of 0.8 at $P \sim 4$ mtorr and gradually decreases with increasing P. $\langle H_2^+\rangle$ gradually decreases with increasing P and $\langle H_3^+\rangle$ increases above $P \sim 10$ mtorr. On the other hand, in case of $T_{vib} = 0$ K, the characteristic of the calculated ion density ratio shows the different tendency as that of the measured ion density ratio. $\langle H^+\rangle$ has no maximum value and gradually decreases with increasing P. In particular, $\langle H_3^+\rangle$ are one-half magnitude smaller than that of measured H_3^+ above $P \sim 8$ mtorr. The value of $\langle n_{H2^+}\rangle$ gradually decreases with increasing P and $\langle n_{H3^+}\rangle$ increases. This discrepancy may be attributed to the fact that the reactions involving H_2, H_2^+ are not vibrationally resolved in the model for solving the system of rate balance equations for ion and gas species. Neglecting vibrational excitation of H_2 would have resulted in a significant underestimation of the molecular ion density in these experiments.

Figure 4 shows the measured the ion densities ratio (H^+, H_2^+, and H_3^+), calculated the ion densities ratio ($\langle H^+\rangle$, $\langle H_2^+\rangle$, and $\langle H_3^+\rangle$) with $T_{vib} = 3000$ K, the electron temperature T_e, and the electron density n_e plotted against discharge current I_d at gas pressure of 8 mtorr. In this condition, n_e increases with increasing I_d, while T_e is nearly constant value of 0.5-1.0 eV and the very bright visible light emission in front of the endplate were observed in the detached plasma. In the low discharge current ($I_d < 40$ A), the measured ion density ratio of H_3^+ is larger than that of H^+. Above $I_d \sim 50$ A, the ion density ratio of H_3^+ is smaller than that of H^+ for the high density plasma. Also, the vibrational resolved model was found to predict the observed dominant ion density ratio.

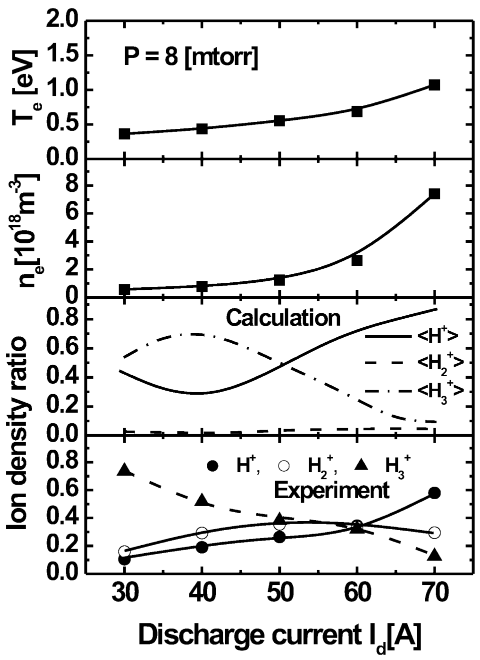

Fig. 4 Measured the ion densities ratio (H^+, H_2^+, and H_3^+), calculated the ion densities ratio ($\langle H^+ \rangle$, $\langle H_2^+ \rangle$, and $\langle H_3^+ \rangle$) with T_{vib} = 3000 K, the electron temperature T_e, and the electron density n_e plotted against discharge current I_d at the gas pressure of 8 mtorr.

4. Conclusion

We have carried out the experimental observation and modeling of molecular ions in hydrogen plasma in a linear plasma device, TPD-SheetIV. From a zero-dimensional model using the relevant rate balance equations, the calculated molecular ion densities of H_2^+, and H_3^+ was found to predict the observed dominant ion density ratio, demonstrating the importance of vibrational temperature of hydrogen molecules. For high density plasma, the effect of molecules on recombination tends to decrease and contributes to assist dissociation and ionization. The conversion of H_2^+ into H_3^+ (CNV2), however, tends to increase and the plasma will contain H_3^+ for low electron temperature using a massive secondary hydrogen gas puffing. Through $H_2(v)$ + H_2^+ or H_3^+ collisions are ignored here, it is conceivable that the creation and destruction of H_2^+ and H_3^+ play a significant role by contribution to the observed high level of $H_2(v)$ internal excitation [4, 9]. Despite the reasonably agreement observed here between our predictions and the experimental data, a need for future modeling to improve understanding of the high level of $H_2(v)$.

Acknowledgments

This work is part of a program supported by the LHD Joint Project, the National Institute for Fusion Science (NIFS04KOBP007) and is partially supported by a Grant-in-Aid No. 18035011 (2006-2007) from the Ministry of Education, Culture, Sports, Science and Technology of Japan.

[1] Post D E, J. Nucl. Mater. **220**–**222**, 143 (1995).
[2] S.I. Krasheninnikov *et al.*, Phys. Lett. A **314**, 283 (1996).
[3] N. Ohno *et al.*, Phy. Rev. Lett. **81**, 818 (1998).
[4] E.M. Hollmann *et al.*, Phys. Plasma **9**, 4330 (2002).
[5] A. Tonegawa *et al.*, J. Nucl. Mater. **313**–**316**, 1046 (2003).
[6] H. Ogawa *et al.*, J. Plasma Fusion Res. SERIES, **6**, 453 (2004).
[7] H. Yazawa *et al.*, Jpn. J. Appl. Phys. **45**, 8208 (2006).
[8] P.C. Stangeby: *The Plasma Boundary of Magnetic Fusion Devices* (Institute of Publishig, Bristol 2000) Chap.l6.
[9] U. Fantz *et al.*, J. Nucl. Mater. **290**–**293**, 367 (2001).
[10] R.K. Janev *et al.*, *Elementary processes in Hydrogen-Helium Plasmas*, ed. G. Ecker, P. Lambropoulos, H. Walther (Springer-Verlag Berlin Heidelberg 1987) Chap.2–Chap.4.
[11] S. Datz *et al.*, Phys. Rev. Lett. **74**, 896 (1995).
[12] A.Yu. Pigarov, Phys. Scr. **T96**, 16 (2006).
[13] P.S. Krstic, Phys. Rev. A **66**, 042717 (2002).
[14] E. Surrey *et al.*, Plasma Phys. Conrol. Fusion **45**, 1209 (2003).
[15] U. Fantz *et al.*, *Franck-Condon Factors Transition Probabilities and Radiative Lifeteimes for Hydrogen Molecules and Their Isotopomeres*, IAEA (2004) INDC(NDS)-457.